AGILE: GIScience Series, 7, 30, 2026. https://doi.org/10.5194/agile-giss-7-30-2026
Proceedings of the 29th AGILE Conference on Geographic Information Science, 16–19 June 2026.
Eds.: Evelyn Uuemaa, Alexander Kmoch, Holger Virro, and Simon Scheider
This contribution underwent peer review based on a full paper submission.


# Monitoring of pesticide treatment effects on crops using optical and SAR satellite remote sensing

Tatjana Kuznecova [1,2], Gustavo Garcia Chapeton [1]

[1] Research group Technologies for Criminal Investigations, Saxion University of Applied Sciences, Enschede, Netherlands
[2] Research group Data Management and Biometrics, University of Twente, Enschede, Netherlands

Correspondence: Tatjana Kuznecova (t.kuznecova@saxion.nl)

**Abstract.** Agricultural chemicals pose increasing risks to soil, water and living organisms. Remote sensing (RS) offers potential to monitor vegetation responses to chemical treatments, yet most existing studies rely on limited samples, optical data only, or controlled experiments. This study explores a plot-level methodology for detecting vegetation responses to herbicide applications in real-world conditions by integrating optical and radar satellite data with pesticide treatment records.

Crop plot geometries and Pesticide Use Reports (PUR) from Kern County, California, served as basis for analysis of RS indices derived from Sentinel-1 Synthetic Aperture Radar (SAR) and Sentinel-2 Multispectral (MS) imagery. The analysis focuses on treatments in potato crops, where a manually enriched pesticide dataset is used to group treatment events by their likely purpose. Two herbicide application scenarios - pre-emergent weed control and vine desiccation - were assessed using slope (1$^{st}$ derivative) and slope-change (2$^{nd}$ derivative) analysis applied to time series of optical and radar indices before and after treatments.

Results show distinct slope and slope-change patterns for both scenarios. Pre-emergent applications exhibit neutral to slightly positive post-treatment trends, while desiccation events are associated with pronounced negative slope changes shortly after treatment. Radar-based metric shows a delayed response compared to optical indices, consistent with differences in spectral and structural vegetation changes.

The findings demonstrate the potential of combining optical and SAR time series with treatment records for large-scale, plot-level assessment of pesticide-related vegetation dynamics. The paper outlines methodological starting points for introducing phenological alignment and control plots to improve causal inference in future work.

**Submission Type.** Analysis

**BoK Concepts.** [PS3] Remote sensing data and imagery, [TA13] EO services and applications, [AM5] Basic analytical methods

**Keywords.** Pesticide effects, Multispectral and SAR integration, change-rate analysis, agricultural crop monitoring

## 1 Introduction

Soils in Europe face growing pressure from contamination by traffic, industry, agriculture, and emerging pollutants such as pharmaceuticals and PFAS (EEA, 2022). At the same time, around 64% of global agricultural lands are at risk of pesticide pollution, including biodiversity-rich areas (Tang et al., 2021). Water quality is equally concerning: recent reports in the Netherlands indicate that up to 96% of measured shallow groundwater locations contain one or more anthropogenic substances, with pesticides among the most common (Arcadis Nederland B.V., 2025). Pesticide spray drifts can damage non-targeted crops and harm living organisms (Albaseer et al., 2025), while improper applications - wrong products, dosages, timing, or use in protected zones such as Natura 2000 areas - pose further risks (Van den Berg et al., 2026; Damalas and Eleftherohorinos, 2011).

Exposure to stressors can cause anomalies in the spectral reflectance of vegetation, potentially detectable through remote sensing technologies. A number of studies assessed crop stress from chemical treatments using remote sensing techniques, in particular from herbicides that can cause crop injury and pose risk of drifts (Bloem et al., 2020; Nehurai et al., 2023; Pause et al., 2019; Suarez, 2018; Yao et al., 2012). While RS techniques can enhance monitoring when combined with advanced statistical methods and Machine Learning techniques (León-lópez et al., 2022; Mouret et al., 2021), the majority of studies are based on small sample sizes or small-scale laboratory or field tests. Furthermore, most focus on optical indices, while integration of other sensor data, such as SAR, is still limited.

Detecting anomalies from chemical treatments is challenging due to variations in crop type, growth stages, environmental conditions and differences in crop sensitivity. Natural factors like drought or activities like mowing can also cause anomalies. Chemical treatments differ in modes of action (selective/non-selective, systemic/contact), purpose (weed control, burndown, desiccation), timing (pre-emergence, post-emergence, pre-harvest), while mixed applications add further complexity. For example, herbicides may either suppress weeds while preserving the crop or intentionally destroy vegetation, as in potato vine desiccation prior to harvest.

Further difficulty is establishing a relevant control sample. Comparing crop plot dynamics without phenological alignment would not lead to reliable conclusions. Hence, identifying suitable features and temporally aligning crop growth cycles to establish comparable treated and untreated groups is an ongoing challenge.

The paper presents methodological starting points illustrated through plot-level slope and slope-change analysis of time series of RS indices before and after treatment events. The study focuses on herbicide applications in two scenarios: a) pre-emergent weed control, b) desiccation of vines.

In the discussion, we also present a future outlook for combining slope analysis with phenological analysis on a plot level to enable comparison of treated and untreated plots.

## 2 Data and methods

A flowchart for processing and analysis steps is included in Appendix 1.

### 2.1 Data

Due to the lack of extensive publicly available datasets in Europe on plot-level pesticide uses, we used open data published by the Kern county in California. It concerns yearly datasets of registered crop plot geometries with crop attributes, together with PUR and permit information. Datasets from 2020–2023 were marked complete at the time of analysis, however the dataset of 2020 was subsequently removed from the official website. Furthermore, Sentinel-1B platform failure in December 2021 lead to more sparse data acquisitions in 2022 and 2023 that may affect the quality of SAR-based analyses. Sentinel-1 and Sentinel-2 imagery was accessed via Google Earth Engine (GEE).

### 2.2 Data preparation

PUR records contain pesticide product names but lack detailed metadata. Therefore, a custom pesticide dataset was compiled by manually enriching reported product names with product type, active ingredients, and typical use (e.g. desiccation, pre-emergent weed control), based on open sources, such as Safety Data Sheets. Most common products were processed, but the registry is not yet complete. PUR records were linked to crop plots by concatenating the attributes *Permit #* and *Site ID*, corresponding to the *PMT_SITE* identifier in the plot geometry dataset.

Only plots with a single crop type (*S_STATUS* = ‘A’) were retained (no multi- or inter-cropping), and plots were assumed to be temporally stable within specified windows before and after treatment events. Analyses were restricted to plots of the target crop (potato), identified using the commodity attribute (*COMM* in plot geometry dataset and *Commodity* in PUR records).

Resulting yearly plot geometries and their attributes served as input to the processing workflow for retrieving satellite data and subsequent statistical analyses.

Two parallel processing workflows were implemented for Sentinel-1 (SAR) and Sentinel-2 (optical MS) data using GEE API in Python, and included image filtering, pre-processing, daily compositing (as a precaution in case of overlapping orbit swaths), computation of RS indices, and extraction of plot-level zonal statistics. Datasets for each analysis year were processed separately.

Sentinel-2 data were obtained from the *COPERNICUS/S2_SR_HARMONIZED* collection, while Sentinel-1 data were retrieved from *COPERNICUS/S1_GRD*, using Interferometric Wide (IW) mode, descending orbit pass, and VV and VH polarizations.

Sentinel-2 pre-processing consisted of cloud masking using Scene Classification Layer (SCL), retaining only vegetation and bare soil classes. Sentinel-1 pre-processing included conversion from dB to linear scale, gamma-nought ($\gamma^0$) correction for incidence angle effects, incident angle filtering (30°-46°), and speckle filtering using Refined Lee method (implementation by (Mullissa et al., 2021)). Full radiometric terrain correction was omitted due to on average negligible terrain slope (<1°).

Within each analysis year, daily median composites were generated for each sensor, whenever imagery was available. From those, various vegetation indices were derived, such as NDVI, EVI, OSAVI, NDRE and others for Sentinel-2, and VH/VV ratio, and RVI for Sentinel-1. Formulas of used indices are presented in Appendix 2. Median zonal statistics were extracted per index, plot and timestamp, alongside valid-pixel fractions, and further reindexed to a daily temporal grid.

Sentinel-1 and Sentinel-2 time series were joined with crop plot attribute data. Only plot-level observations with valid-pixel fractions > 0.3 were retained. Missing observations due to irregular revisit intervals were filled using linear interpolation (up to 17 consecutive days) and time series were trimmed to remove trailing missing values at the start or end of the series. Time series that were still incomplete were discarded. Remaining time series were lightly smoothed using a Savitzky–Golay filter (*SciPy* library, window size 21, order 2).

### 2.3 Analysis

Vegetation responses to pesticide treatments were analysed by using slope (1st derivative) and slope-change (2nd derivative) values calculated from time series of multiple optical and radar indices within fixed temporal windows. Slopes were derived by fitting linear trends (*NumPy polyfit*, *1st degree*) to RS indices within five intervals of 7-day width before and after the treatment dates. Slope changes were calculated as slope differences between consecutive intervals and normalized by interval width. Treatments were processed as independent events, although multiple sequential treatments may occur in the same plot. Interdependencies between treatments should be considered in future research.

The treated area share for each plot was calculated from PUR attributes dividing treated area by planted area. Only treatments covering more than 80% of planted area were retained.

As PUR records do not specify treatment purpose, treatments were grouped into scenarios based on assumptions informed by common agricultural practices and supported by visual examination of the time series. Potential vine desiccation cases were inferred from the use of typical active substances like *Carfentrazone-ethyl, Diquat, Glufosinate, Pyraflufen-ethyl* applied at higher NDVI values (> 0.5). Whereas, pre-emergent weed control treatments assumed the use of *Dimethenamid-P, EPTC, Flumioxazin, Oxyfluorfen, Pendimethalin, S-metolachlor, Trifluralin* applied at low NDVI values (0 to 0.25). List of substances may still be incomplete, and thresholds are currently roughly defined for exploratory purposes. Furthermore, cases of mixed pesticide applications were allowed (e.g. herbicide and insecticide combinations).

### 2.4 Data and Software Availability

The code for data processing and analysis workflows is not publicly released due to ongoing research, but will be made available after completion of follow-up studies. Methodology section includes sufficient details to allow reproducibility. Code snippets may be made available on reasonable request. Public datasets of the Kern county can be obtained from the official website: http://www.kernag.com/gis/gis-data.asp. Part of the Sentinel-1 processing workflow includes a script by (Mullissa et al., 2021) from: https://github.com/adugnag/gee_s1_ard.

## 3 Results

Slope and slope-change values per interval are aligned by treatment date and presented in a form of box-and-whiskers plots (Fig. 1 and Fig. 2), where medians and outliers above 0 are shown in green colour, and below 0 - in red colour. Due to obvious correlation between some of the indices, we present only a subset of all analysed indices: NDVI, EVI, NDRE (version with B6 band) and RVI.

For pre-emergent herbicide applications (521 cases; Fig. 1), optical indices exhibit very similar patterns, except NDRE(B6). Neutral pre-treatment slopes with predominantly negative outliers indicate that treatments, expectedly, are applied after crop decline or in-between growth cycles. Post-treatment slopes are slightly positive with a gradual slope increase without significant jumps in slope-change values. This appears consistent with the intended effect of pre-emergence herbicides, which suppress weed germination without affecting existing vegetation. NDRE(B6) and RVI exhibit smaller median changes but a wider spread, likely reflecting greater susceptibility to noise. Strong post-treatment outliers in slopes and slope changes may warrant further investigation, as they may reflect treatment inconsistencies or application differences.

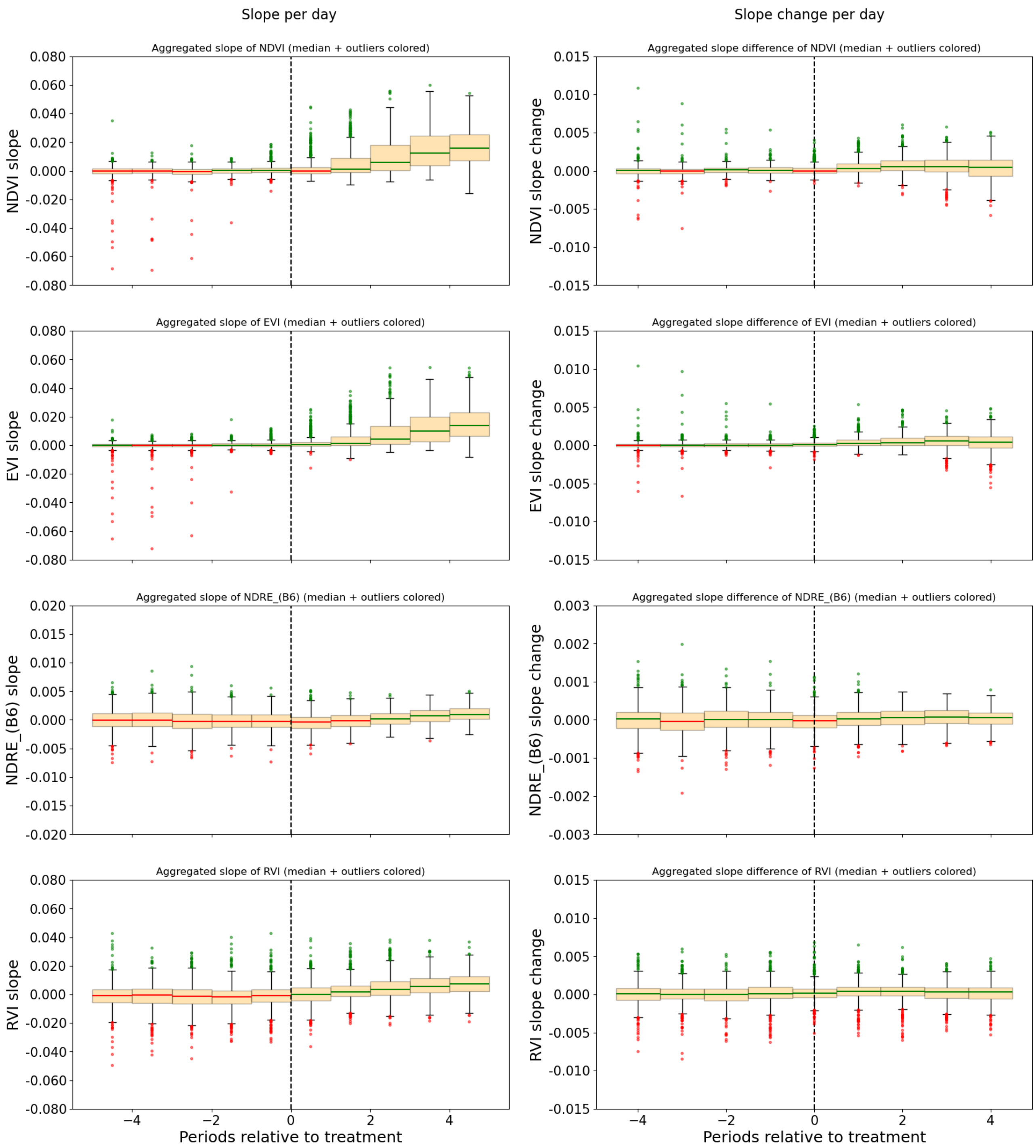


**Figure 1.** Potential pre-emergent applications with NDVI at the time of treatment between 0 and 0.25: slope (left) and slope change (right), 2020-2023, 521 cases.

For desiccant applications (157 cases; Fig. 2), all indices show negative slope trends in the post-treatment intervals. Decline in most optical indices already starts before treatment, which is not surprising, since desiccation is usually performed after the crop reaches maturity (onset of natural senescence). However, slopes drop significantly further immediately after application and stabilize near zero in later intervals, consistent with near-complete vegetation die-out. Post-treatment slope outliers are predominantly negative, indicating extreme vegetation decline in some cases. Difference in response between NDRE(B6) and other optical indices may be interesting to explore further, as it may reveal differences between early chlorophyll loss and canopy structural loss.

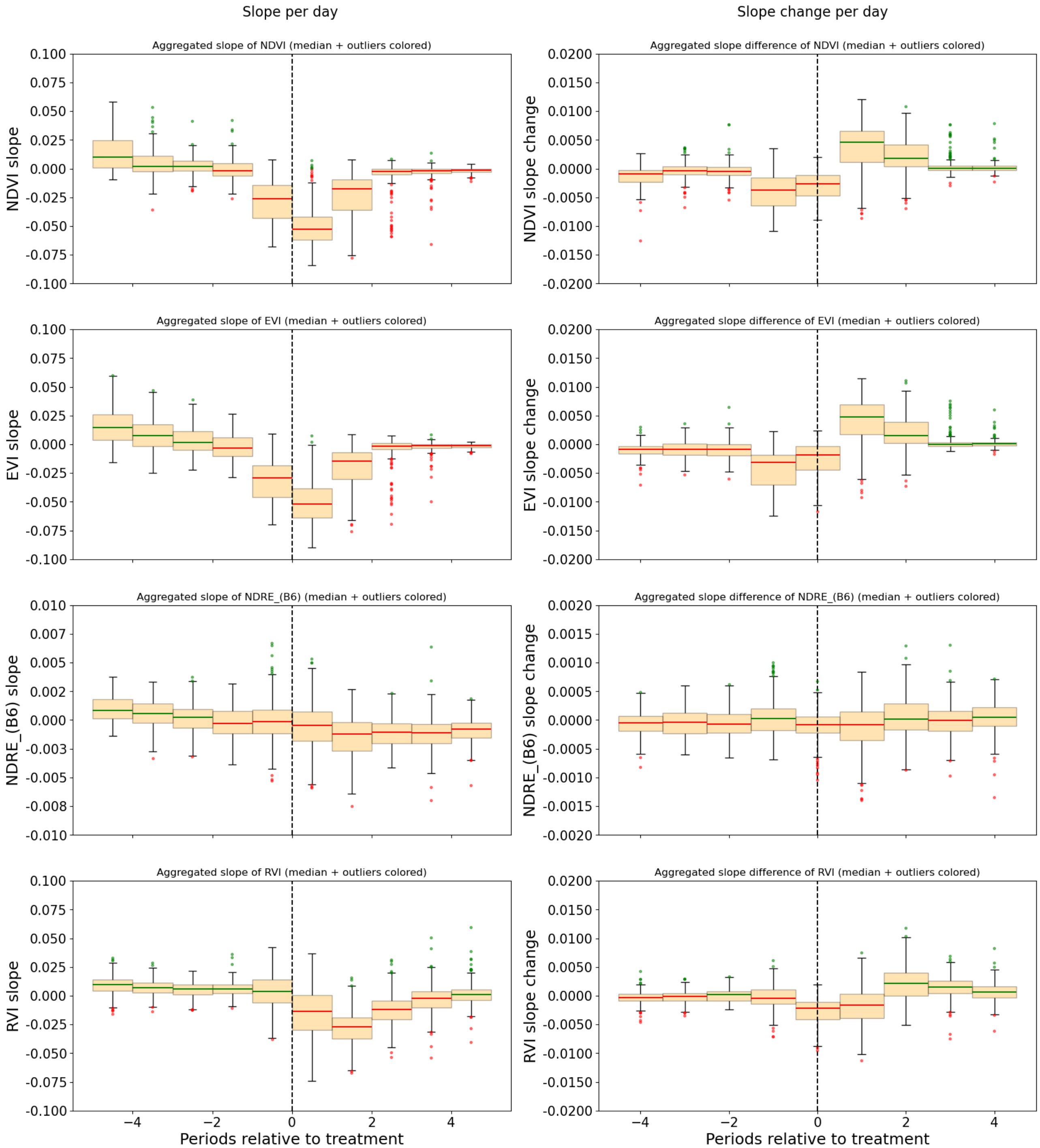


**Figure 2.** Desiccant application cases with NDVI at the time of treatment between 0.5 and 1: slope (left) and slope change (right), 2020-2023, 157 cases.

RVI on average does not drop till after the treatment and overall exhibits a delayed post-treatment decline compared to optical indices. This temporal offset seems consistent with scenarios where spectral changes (e.g. yellowing) precede structural degradation. This provides some positive evidence that combination of optical and radar indices may prove useful in discerning different types of stresses or interventions in the future.

## 4 Discussion and conclusions

The paper presents a preliminary analysis of potential chemical treatment effects in potato crops at plot level, using optical and radar indices derived from Sentinel-1 and Sentinel-2 data. Two distinctive treatment scenarios were used as illustrative cases: a) pre-emergence treatments and b) vine desiccation, demonstrating the diversity of effects expected from different types and timings of treatments. Notably, the RVI index showed a delayed response compared to optical indices in desiccant applications, supporting complementarity of optical and radar indices, which will be explored further in follow-up research.

Current approach enables tracking of short-term vegetation responses at plot level, but does not yet include an explicit control group. Asynchronous, crop-specific growth dynamics make direct plot comparison challenging. To address this, future research will combine phenological analysis with slope analysis. Extracting key phenological milestones from reference time series (e.g. NDVI) and deriving growth cycle characteristics – growth season length, growth and decline periods and change rates - can enrich analysis of treatment events. Slope analyses of RS indices aligned by likely phenological stages can further enable comparison across treatment scenarios and between treatment and control groups.

The analysis is sensitive to preprocessing approaches, particularly temporal smoothing, which can obscure subtle changes in RS indices. Additionally, PUR records do not include information on purpose of treatments, therefore scenario-based grouping relied on assumptions. Plot size, ranging from ~ 5 to 450 acres in analysed plots, was not considered as a factor. These and other details may be refined in the future.

Overall, the presented results should be interpreted as methodological exploration rather than definitive attribution of treatment effects, providing a foundation for more robust comparative analyses in follow-up studies.

## Declaration of Generative AI in writing

The authors declare that they have used Generative AI tools in the preparation of this manuscript. Specifically, the AI tools were utilized for language editing, improving grammar, sentence structure, and code editing, but not for generating scientific content, research data, or substantive conclusions. All intellectual and creative work, including the analysis and interpretation of data, is original and has been conducted by the author without AI assistance.

## Author contribution

Conceptualization: TK, GG; Data curation: TK; Formal analysis: TK; Methodology: TK, GG; Investigation: TK; Software: TK, GG; Visualization: TK; Validation: TK; Writing – original draft, review & editing: TK, GG.

## References


Albaseer, S. S., Jaspers, V. L. B., Orsini, L., Vlahos, P., Al-Hazmi, H. E., and Hollert, H.: Beyond the field: How pesticide drift endangers biodiversity, Environmental Pollution, 366, 125526, https://doi.org/10.1016/j.envpol.2024.125526, 2025.

Arcadis Nederland B.V.: Grondwaterkwaliteit Nederland 2024, 2025.

Van den Berg, S., Droge, S., Holterman, H.-J., and Buddendorf, B.: Pesticiden in terrestrische Natura 2000-gebieden. Verkennende beoordeling op aanwezigheid, blootstellingsroutes en potentiële ecologische risico's voor bodemorganismen en niet-doelwit geleedpotigen., Wageningen, https://doi.org/https://doi.org/10.18174/708361, 2026.

Bloem, E., Gerighausen, H., Chen, X., and Schnug, E.: The potential of spectral measurements for identifying glyphosate application to agricultural fields, Agronomy, 10, https://doi.org/10.3390/agronomy10091409, 2020.

Damalas, C. A. and Eleftherohorinos, I. G.: Pesticide exposure, safety issues, and risk assessment indicators, Int. J. Environ. Res. Public Health, 8, 1402–1419, https://doi.org/10.3390/ijerph8051402, 2011.

EEA: Soil monitoring in Europe - Indicators and thresholds for soil health assessments, Luxembourg, https://doi.org/10.2800/956606, 2022.

León-lópez, K. M., Member, S., Mouret, F., Arguello, H., and Member, S.: Anomaly Detection and Classification in Multispectral Time Series Based on Hidden Markov Models, IEEE Transactions on Geoscience and Remote Sensing, 60, https://doi.org/10.1109/TGRS.2021.3101127, 2022.

Montero, D., Aybar, C., Mahecha, M. D., Martinuzzi, F., Söchting, M., and Wieneke, S.: A standardized catalogue of spectral indices to advance the use of remote sensing in Earth system research, Sci. Data, 10, 1–20, https://doi.org/10.1038/s41597-023-02096-0, 2023.

Mouret, F., Albughdadi, M., Duthoit, S., Kouamé, D., Rieu, G., and Tourneret, J. Y.: Outlier detection at the parcel-level in wheat and rapeseed crops using multispectral and sar time series, Remote Sens. (Basel)., 13, 1–25, https://doi.org/10.3390/rs13050956, 2021.

Mullissa, A., Vollrath, A., Odongo-Braun, C., Slagter, B., Balling, J., Gou, Y., Gorelick, N., and Reiche, J.: Sentinel-1 sar backscatter analysis ready data preparation in google earth engine, Remote Sens. (Basel)., 13, 5–11, https://doi.org/10.3390/rs13101954, 2021.

Nehurai, O., Atsmon, G., Kizel, F., Kamber, E., Bar, N., Eizenberg, H., and Lati, R. N.: Early detection of the herbicidal effect of glyphosate and glufosinate by using hyperspectral imaging, Agron. J., 115, 2558–2569, https://doi.org/10.1002/agj2.21415, 2023.

Pause, M., Raasch, F., Marrs, C., and Csaplovics, E.: Monitoring glyphosate-based herbicide treatment using Sentinel-2 time series-A proof-of-principle, Remote Sens. (Basel)., 11, https://doi.org/10.3390/rs11212541, 2019.

Suarez, L. A.: Proximal and Remote Sensing for Early Detection and Assessment of Herbicide Drift Damage on Cotton Crops, PhD thesis, University of Southern Queensland, 202 pp., 2018.

Tang, F. H. M., Lenzen, M., McBratney, A., and Maggi, F.: Risk of pesticide pollution at the global scale, Nat. Geosci., 14, 206–210, https://doi.org/10.1038/s41561-021-00712-5, 2021.

Yao, H., Huang, Y., Hruska, Z., Thomson, S. J., and Reddy, K. N.: Using vegetation index and modified derivative for early detection of soybean plant injury from glyphosate, Comput. Electron. Agric., 89, 145–157, https://doi.org/10.1016/j.compag.2012.09.001, 2012.

# Appendix 1

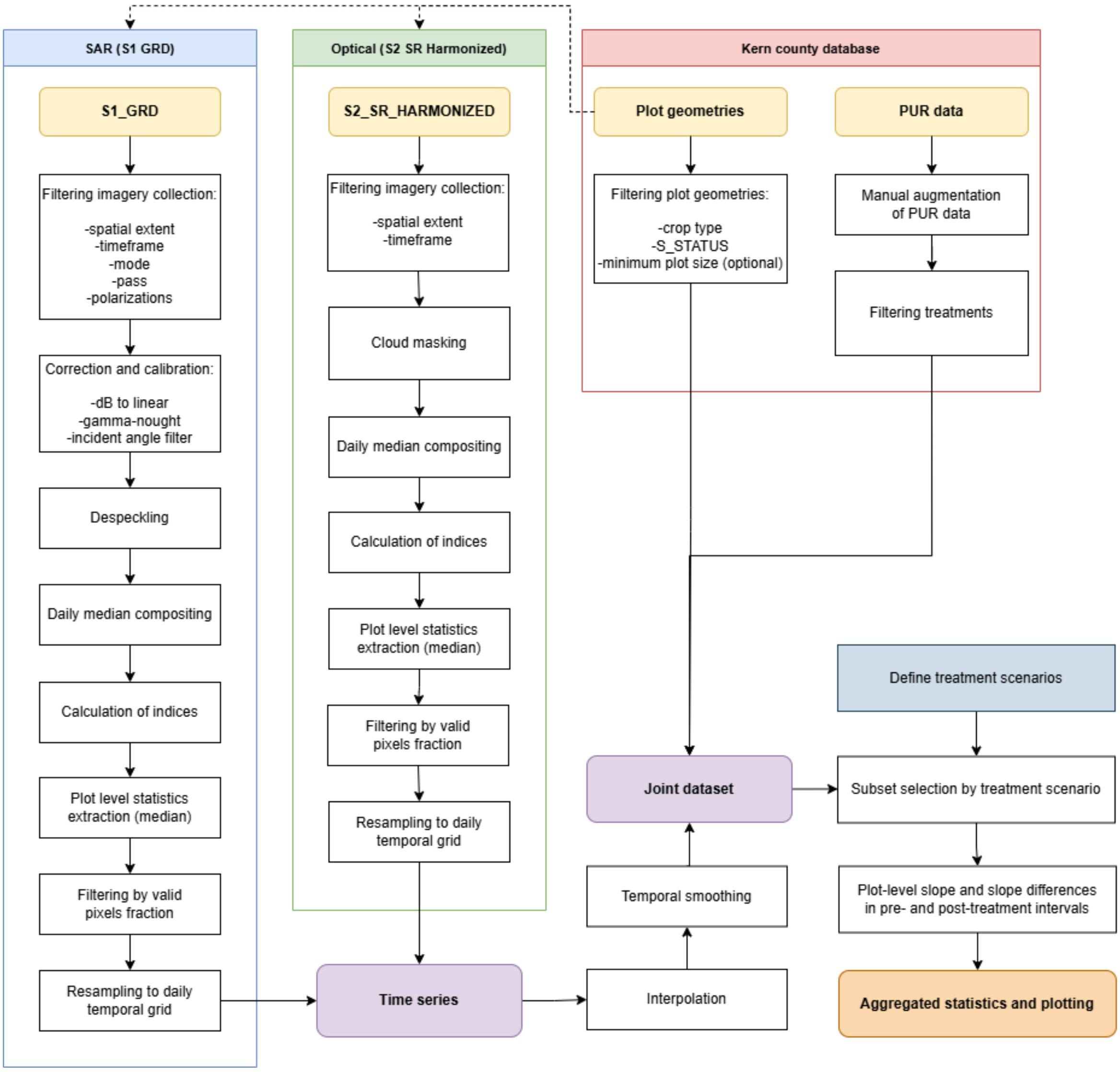


**Figure 3.** Processing flowchart

## Appendix 2

Table 1. Remote sensing indices used in the paper. For convenience, we refer to Awesome Spectral Indices database (Montero et al., 2023).

| Index name | Acronym | Formula |
|---|---|---|
| Enhanced Vegetation Index | EVI | $EVI = 2.5 * (\frac{B8 - B4}{B8 + 6 * B4 - 7.5 * B2} + 1))$<br>Sentinel-2 bands:<br>B8: NIR<br>B4: Red<br>B2: Blue |
| Normalized difference vegetation index | NDVI | $NDVI = \frac{B8 - B4}{B8 + B4}$<br>Sentinel-2 bands:<br>B8: NIR<br>B4: Red |
| Normalized Difference Red Edge Index (version with B6 band) | NDRE/ NDREI | $NDRE = \frac{B8 - B6}{B8 + B6}$<br>Sentinel-2 bands:<br>B6: Red Edge 2<br>B8: NIR |
| Optimized Soil Adjusted Vegetation Index | OSAVI | $OSAVI = \frac{B8 - B4}{B8 + B4 + 0.16}$<br>Sentinel-2 bands:<br>B8: NIR<br>B4: Red |
| Radar Vegetation Index | RVI/ DpRVIVV | $RVI = \frac{4 * VH}{VV + VH}$<br>Dual-pol version for Sentinel-1. |